

# Platelet adhesion and aggregate formation controlled by immobilised and soluble VWF

**Matthias F. Schneider**

Technical University Dortmund, Department of Physics

**Mohammad A. Fallah**

University of Konstanz, Department of Chemistry

**Christian Mess**

University Medical Centre Hamburg-Eppendorf

**Tobias Obser**

University Medical Centre Hamburg-Eppendorf

**Reinhard Schneppenheim**

University Medical Centre Hamburg-Eppendorf

**Alfredo Alexander-Katz**

Massachusetts Institute of Technology

**Stefan W. Schneider**

University Medical Centre Hamburg-Eppendorf

**Volker Huck** (✉ [v.huck@uke.de](mailto:v.huck@uke.de))

University Medical Centre Hamburg-Eppendorf <https://orcid.org/0000-0001-8988-1091>

---

## Research article

**Keywords:** von Willebrand factor, platelet adhesion, shear activation, primary haemostasis

**Posted Date:** March 12th, 2020

**DOI:** <https://doi.org/10.21203/rs.3.rs-16888/v1>

**License:**  This work is licensed under a Creative Commons Attribution 4.0 International License.

[Read Full License](#)

---

**Version of Record:** A version of this preprint was published on September 11th, 2020. See the published version at <https://doi.org/10.1186/s12860-020-00309-7>.

# Abstract

**Background** It has been demonstrated that von Willebrand factor (VWF) mediated platelet-endothelium and platelet-platelet interactions are shear dependent. The VWF's mobility under dynamic conditions (e.g. flow) is pivotal to platelet adhesion and VWF-mediated aggregate formation in the cascade of VWF-platelet interactions in haemostasis.

**Results** Combining microfluidic tools with fluorescence and reflection interference contrast microscopy (RICM) microscopy, here we show, that specific deletions in the A-domains of the biopolymer VWF affect both, adhesion and aggregation properties independently. Intuitively, the deletion of the A1-domain led to a significant decrease in both adhesion and aggregate formation of platelets. Nevertheless, the deletion of the A2-domain revealed a completely different picture, with a significant increase in formation of rolling aggregates (gain of function). We predict that the A2-domain effectively 'masks' the potential between the glycoprotein Ib and the A1-domain. Furthermore, the deletion of the A3-domain led to no significant variation in either of the two functional characteristics.

**Conclusions** These data demonstrate that the macroscopic functional properties i.e. adhesion and aggregate formation cannot simply be assigned to the properties of one particular domain, but have to be explained by cooperative phenomena. The absence or presence of molecular entities likewise affects the properties (thermodynamic phenomenology) of its neighbours, therefore altering the macromolecular function.

## Background

The shear dependent role of von Willebrand factor (VWF) during primary haemostasis is very well established and investigated (1–10). Furthermore, both qualitative (Type II) and quantitative (Type I and III) VWF variants are classified in the framework of von Willebrand disease (VWD) (11–13). VWD as a hereditary disease is a common bleeding disorder caused by mutations of VWF resulting in deficiency or dysfunction of this biopolymer.

In addition, the acquired von Willebrand factor syndrome (AVWS), reviewed by Tiede and coworkers, subsumes diverse non-inherited qualitative, structural or functional VWF disorders resulting in an enhanced risk of bleeding (14, 15). The hereditary VWD certainly affects both the immobilised and the soluble VWF fractions, whereas AVWS leads to an impact only on the mobile fraction. Although the first step of haemostasis depends on the presence of an intact immobilised binding partner for platelets in the subendothelial vessel wall (16–18), bleeding episodes of patients suffering from AVWS illustrate that the mobile VWF fraction is a prerequisite for an effective VWF triggered blood clotting. Independent of the different pathomechanisms and clinical manifestations, the similar symptomatic therapeutic regimens of these syndromes underline the central role of VWF's functional characteristics.

Former studies on single VWF molecules under flow (9, 19) as well as on its collective behaviour (20, 21) have further elucidated the role of VWF while in motion. Large VWF-platelet-aggregates of several 100  $\mu\text{m}$

in size, formed reversibly above a critical shear threshold, begin to roll on the surface of a microfluidic channel under whole blood conditions (22, 23). These data demonstrate once more the importance to approach blood clotting as a dynamic process, in which in general important conformations - or better states - of all contributing constituents are a function of all physical (here shear flow) and biochemical (e.g. pH, multimer size) conditions.

In this study, we combined a microfluidic setup with fluorescence- and reflection interference contrast microscopy (RICM) to compare the impact of various deletions on VWF's A-domain on the physiological function of both immobilised and soluble VWF. Systematically deleting the A1-, A2- or A3-domain of the surface-bound (immobilised) and mobile (soluble) VWF fraction, while studying platelet adhesion and reversible VWF-platelet aggregate formation over a wide range of shear rates, revealed the non-trivial interrelation between these domains, and showed that similar adhesion characteristics can be accompanied by a significant shift in aggregation tendency depending on the specific mutation.

## Results

### A. Platelet adhesion on immobilised VWF

Focusing on the shear conditions present in the human microvasculature (24) we applied shear rates between  $500 \text{ s}^{-1}$  and  $10,000 \text{ s}^{-1}$ . Figure 2 plots the adhesion of platelets under low shear conditions as a function of time for the three different VWF A-domain deletion variants (del-A1, del-A2, del-A3) in the absence of soluble VWF. Whereas biofunctionalisation with wt VWF led to a time-dependent increase in platelet adhesion, coating with del-A1 VWF mutant failed to bind platelets, comparable to biofunctionalisation with bovine serum albumin (BSA) serving as negative control. Albeit the complete deletion of entire subdomains, there was no significant difference between del-A3 and wt VWF. The slight change of platelet adhesion to del-A2 remained negligible compared to the wildtype glycoprotein. These platelet adhesion characteristics were quantified by the SC of platelets at the footprint of the biofunctionalised channels relative to wt VWF as previously published (25) (see Fig. 2b).

Keeping the immobilised VWF fraction unchanged, we next addressed the role of soluble VWF in the process of platelet adhesion. Therefore, we performed flow experiments on channels biofunctionalised with wt VWF, with or without addition of mobile wt VWF at distinct shear rates in the range of  $1,000 \text{ s}^{-1}$  to  $10,000 \text{ s}^{-1}$ . As shown in Fig. 3, there were no qualitative differences between these experimental groups regarding the platelet SC at low shear rates (Fig. 3a). But interestingly, at higher shear rates platelets could only adhere to the immobilised VWF in the presence of soluble VWF (Fig. 3b and c). These data illustrate that the mobile VWF fraction is a prerequisite for platelet adhesion under high shear conditions.

### B. Collective behaviour: mobile VWF-induced aggregate formation

Recently we could show that under whole blood conditions large VWF-platelet aggregates reversibly formed above a critical shear threshold rolling alongside the surface of a microfluidic channel (22, 23).

For the process of rolling aggregate formation see Fig. 4 and the RICM time-lapse live-cell movie (Additional file 1).

In Fig. 5a, a sequence of images along increasing shear rates is shown, where in addition to surface-bound immobilised VWF, VWF was also present in solution (mobile). Deletions of an individual domain showed distinct consequences on the aggregate formation: While A1-deletion mutant completely failed to induce VWF-platelet aggregates on an intact wt VWF biofunctionalised surface, the A2- and A3-deletion mutants are capable of aggregate formation. Compared to addition of wt VWF, del-A2 formed aggregates even at lower shear rates, clearly indicating a gain of function. A meaningful quantitative measure of aggregate formation has been shown to be the critical shear rate ( $\dot{\gamma}_{crit}$ ), which in principle determines a nucleation point (20). To quantify  $\dot{\gamma}_{crit}$  next to the optical identification of first rolling aggregates (see Fig. 5a, red circles), we plotted the RICM signal intensities of aggregated platelets against the time, here representing distinct shear rates (Fig. 5b). Maximum fluctuations in the intensity plots correspond to  $\dot{\gamma}_{crit}$ .

## Discussion

In this study, it was clearly shown that, in order to determine the influence of VWF in the first step of haemostasis, solely the quantification of the platelet adhesion – using in vitro standard procedures – is not sufficient. Only the comprehension of the biophysical component of the fluid dynamics on the one hand, the integration of both collective and single molecule phenomena on the other hand, and finally the distinction between immobilised and soluble VWF opens up the possibility for a targeted investigation of the mechanistic background.

Platelet adhesion on immobilised VWF is a time dependent process. To study the initial step of platelet adhesion due to interactions of the VWF A1-domain and the platelet glycoprotein (GP) Ib, platelet activation was inhibited as previously described (26). Thus, platelet derived VWF was excluded as a further source of the mobile VWF fraction. As expected, biofunctionalisation with the deletion mutation del-A1 succeeded in coating but completely failed to bind platelets. Regarding the platelet adhesion capability on immobilised VWF, the deletion mutations del-A2 and del-A3 did not show any significant variation compared to wt VWF. As bleeding events are known to cause pathological high-shear conditions in the area directly affected by the damaged vessel (27), we next focused on short-termed VWF-platelet interactions upon different shear flow regimens. Under low- or intermediate-shear conditions, the impact of the mobile VWF fraction on platelet adhesion to VWF biofunctionalised surfaces was negligible. Nevertheless, in the entire absence of soluble VWF, platelet binding to the surface was significantly diminished upon high shear application (see Fig. 3). In contrast, in the presence of soluble VWF rising shear led to an enhanced platelet adhesion. In accordance with former publications (28, 29), platelet decorated strings appear within seconds (see Electronic Supplementary Material 1), most likely due to a recruitment of stretched mobile VWF to the platelet surface.

Although single platelet adhesion to the channel footprint and consecutive recruitment of soluble VWF are the likely prerequisites for aggregate formation, adhesion characteristics have no predictive power for

the formation of rolling VWF-platelet aggregates. As shown for the selected deletion variants of the A-subdomains of VWF, a deletion of the A1-domain indeed led to a significant decrease in adhesion and a complete loss of aggregate formation. Nevertheless, while the impact of the A3-domain on adhesion and aggregate formation seemed to be marginal, a deletion of the A2-domain – although leading to a negligible change in platelet adhesion – induced a significant reduction in  $\dot{\gamma}_{crit}$ , i.e. an increase in the formation of VWF-platelet aggregates. Note that due to the absence of divalent cations during the whole course of microfluidic experiments, the activity of the VWF degradation enzyme ADAMTS-13, known to specifically interact with the VWF A2-domain, is inhibited to facilitate the concentration on the VWF interdomain affection. Although one could raise the hypothesis that adhesion and aggregate formation are regulated by specific binding sites on different parts along the molecule (e.g. the collagen binding site of the A3-domain) (30, 31), we here prefer to look at this molecule from a different more physical angle:

Our results strongly support a hypothetical scenario suggested earlier by Ruggeri et al. (6): Single platelets tethered to immobilised VWF function as nucleation centres. Soluble VWF binds to the immobilised platelet, in particular under high shear flow, thereby representing a nucleation centre itself supporting the growth of the aggregate. The aggregate formation can be explained by a three-step process and the “matching” of two timescales. First, the elongational contribution of the shear field supports the elongated state of VWF (Fig. 6a). The shear field also introduces the first timescale

$\tau_{rot} \approx l / \dot{\gamma}$  (gamma representing the shear rate), the period of one rotation of a platelet exposed to the field. The second timescale  $\tau_{bind}$  arises from the binding kinetics and corresponds to the time the elongated VWF typically resides on the platelet. Of course, in reality, all these quantities are thermodynamic quantities and will vary with temperature, pH, ion concentrations etc. in other words they are represented by their appropriate diagrams of state (32). Nevertheless, if  $\tau_{rot} \ll \tau_{bind}$  the VWF will reside long enough on the platelet to wrap around it (Fig. 6b). This will effectively coat the platelets due to the enlarged contact area. Via VWF-VWF interactions the platelets can now begin to form aggregates, given a high enough concentration of platelets (Fig. 6c).

We must note that a recent work explaining how VWF adheres to surfaces at high shear rates can also be used to explain why aggregate formation occurs only in the presence of soluble VWF (33). In particular, at shear rates above  $1,000 \text{ s}^{-1}$ , platelets are exposed to shear forces in the range above of 10 pN. This force is around the rupturing force of the GPIb-A1 bond (34). Thus, in excess of this force platelets need a cooperative mechanism to bind. By forming aggregates, it is possible to overcome this limit since the binding to the substrate leads to a higher valence arising from the other platelets on the string. As long as the lifetime of the bonds is long enough, such aggregates will be able to bind and immobilise on the substrate.

The gain of function observed during aggregate formation for the del-A2 mutations reveals that the simple picture of altered VWF-platelet association (Fig. 2) leads to a false prediction of the aggregation behaviour. As shown in Fig. 5, the threshold shear rate at which aggregates form for wt VWF is of the order of  $4,000 \text{ s}^{-1}$ ; however, in the case of the deletion of the A2-domain it is  $2,500 \text{ s}^{-1}$ . The  $\sim 40\%$

change in this threshold shear rate can be accounted by an increase in the binding strength between the A1-domain and the platelet GPIb receptor. As has been previously speculated, we can confirm that the GPIb-A1 interaction is regulated by the presence of the A2-domain (21, 35). It is believed that the interaction is masked by the A2-domain yielding an effective lifetime of the GPIb-A1 bond that displays a “catch-bond” behaviour (36–38). In the absence of the A2-domain, the lifetime at lower shear forces of the GPIb-A1 bond was radically increased. By how much? Based on our previous work on aggregate formation (20), it is possible to measure such differences. In particular, in order to reduce the critical shear rate by  $x$ , the lifetime of the GPIb-A1 has to increase by the same factor  $x$ . By assuming that all prefactors remain the same, we find that the effective interaction strength between the GPIb and the A1-domain has to increase by  $\sim 1 kT$ , where  $k$  is the Boltzmann constant and  $T$  the temperature.

Such variation is small, yet has a dramatic impact on the clotting process. Thus, we predict that the A2-domain effectively “masks” the potential between the GPIb and the A1-domain by about  $1 kT$ . While it would be hard to resolve, this change should not carry over into the high shear regimen as the shear forces will already be enough to pull apart the domains and reduce the masking ability of the A2-domain.

## Conclusions

The results of our in vitro study contribute to a deeper understanding of the stepwise process of VWF activation and further clarify the impact of mobile VWF-initiated aggregate formation in the cascade of VWF-platelet interactions. Taken together, these findings call for a thermodynamic approach to understand VWF triggered blood clotting where the mechanical perspectives recently discovered (9, 39–43) are only a way towards an integrative perspective. In future, therefore it will be necessary to extract the phenomenology of VWF, here the changes of the protein’s state upon deletion mutations, by experiments, which are analysed thermodynamically and are the basis of a physical explanation of biological function as well as a gain to new insight on a microscopic scale.

## Methods

### A. Microfluidic channel system

The fluid dynamic conditions of the human microvasculature, was mimicked in a pneumatically driven microfluidic channel system (BioFlux, San Francisco, California, USA). The BioFlux system is a bench-top instrument, which allows long-term temperature-controlled flow cell assays. Its pressure interface connects a high precision electropneumatic pump to the well plates to initiate controlled flow rates with a nominal shear rate precision of  $36 \text{ s}^{-1}$ . The channel geometry is a straight rectangular duct with a width of  $350 \mu\text{m}$  and a height of  $75 \mu\text{m}$ . Biofunctionalisation succeeded by coating the channels with either wild-type von Willebrand factor (wt VWF) or a deletion mutant VWF in a concentration of  $50 \mu\text{g/ml}$  each. A homogenous coating, representing the immobilised VWF at the extracellular matrix of a subendothelial vessel wall, was achieved after incubation over night at  $37 \text{ }^\circ\text{C}$  in a moisture rich environment as previously published (20).

## B. Microscopic setup

The microfluidic channel system was mounted onto an inverted microscope (Zeiss Axio Observer Z.1, Zeiss AG, Oberkochen, Germany) operated in either fluorescence- or RICM-mode, respectively. RICM is especially beneficial for studying both dynamic and static biological phenomena taking place in vicinity of a transparent substrate, especially under whole blood experimental conditions. This microscopy mode is used to study the interference pattern of polarised incoming light being reflected at an object in order to reconstruct the height profile of the object at an interface. Briefly, the interference of the object beam and the reference beams results in an image with information on the height profile of the sample. For reduction of scattered light, we utilise the antiflex technique, in which the incident light passes a linear polariser. Consequently, the RICM technique assures detection of the platelet membrane coming in direct contact with the observed surface in a high spatial resolution (44). A sketch of this setting is shown in Figure 1. Image acquisition was performed using a CCD camera (AxioCam MrM) and ZEN software (both Zeiss AG, Jena, Germany).

## C. Cell culture and expression of recombinant wildtype and deletion mutant VWF

For recombinant VWF expression, we used HEK293 cells. Cells were cultured in Dulbecco Modified Eagle Medium (DMEM, Invitrogen, Karlsruhe, Germany) with 10% foetal bovine serum and 1% penicillin/streptavidin at 37°C. Then, cells were transfected with Lipofectamine 2000 (Invitrogen, Karlsruhe, Germany) and VWF-plasmid-constructs in vector pIRESneo2. Recombinant expression of VWF variants was performed as previously described. In brief, HEK293 cells stably express wt VWF or indicated deletion mutants. Samples of the supernatant were taken after 72 hours, centrifuged (5 min at 270 g, 4°C) and concentrated with Amicon Ultrafree-15. The VWF concentration was determined by VWF:Ag-ELISA.

## D. Preparation of the perfusion media

For preparation of the perfusion media, blood was smoothly collected from healthy volunteers after informed consent. We utilised sodium citrated monovettes with manual syringe stamps to avoid platelet preactivation and further inhibit the activity of inherent degradation enzymes (e.g. ADAMTS-13). This study was conducted in conformity to the *Declaration of Helsinki* (45) and to *The International Conference on Harmonisation of Technical Requirements for Registration of Pharmaceuticals for Human Use (ICH)* Guidelines available at <http://www.ich.org>. It was approved by the Ethics Committee II of the Heidelberg University (Mannheim, Germany).

Platelets were isolated from blood samples, washed and fluorescently stained as previously published (26). These platelets were resuspended in divalent cation free phosphate-buffered saline solution and used for perfusion in a concentration of 200,000 per  $\mu\text{l}$  supplemented with 45% haematocrit. Alternatively, the blood samples were natively perfused as whole blood supplemented with wt VWF or deletion mutant VWF as indicated.

## E. Experimental procedure

Under physiological conditions, VWF comes into effect in both the extracellular matrix of the subendothelial vessel wall (immobilised) and the circulating plasma (soluble) (4, 6-8). Three sets of experiments were designed to discretely mimic the complex physiology of VWF mediated platelet adhesion and VWF-platelet aggregate formation *in vitro*:

1. In order to investigate the impact of deletions in the VWF A-domains on platelet adhesion, microfluidic channels were biofunctionalised with indicated deletion mutant VWF and perfused with washed platelets supplemented with 45% haematocrit as described above at a shear rate of  $500 \text{ s}^{-1}$ . After 1, 5 and 10 minutes of perfusion, platelet adhesion was studied by fluorescence microscopy using a Zeiss 10fold objective compared to platelet adhesion on wt VWF biofunctionalisation. Note that no soluble VWF was present in these experiments.
2. Addressing the impact of immobilised and soluble VWF on platelet adhesion under physiological and pathological flow conditions, channels were biofunctionalised with wt VWF. Then, we perfused the channels with the washed platelet solution supplemented with 45% haematocrit as described above with or without addition of  $10 \mu\text{g/ml}$  wt VWF. Perfusion was performed at distinct shear rates in the range of  $1,000 \text{ s}^{-1}$  to  $10,000 \text{ s}^{-1}$  for 5 minutes. Live cell fluorescence videos were recorded with four frames per second using a Zeiss 20fold objective and analysed as described.
3. To study VWF-platelet aggregate formation, channels were biofunctionalised with wt VWF as described above. The biofunctionalised channels were perfused with native whole blood, additionally supplemented with indicated A-domain deleted VWF thus raising the collective VWF concentration to  $50 \mu\text{g/ml}$ . The aggregation behaviour, namely the critical shear rate necessary for the formation of VWF-platelet aggregates, was then monitored as previously published (20). Briefly, the shear rate was consecutively increased from  $1,000 \text{ s}^{-1}$  to  $5,000 \text{ s}^{-1}$  in discrete steps for 30 seconds each, and RICM movies were recorded with two frames per second using a specialised Zeiss 63fold antilex objective. VWF-platelet aggregates consisting of at least 15 platelets rolling at the channel footprint were considered rolling aggregates. We determined the critical shear rate for formation of these whole blood/A-domain deleted VWF aggregates compared to those of whole blood supplemented with wt VWF. For each experiment of the aforementioned settings at least four independent experiments were performed.

## F. Image analysis and statistical computation

For image analysis, we used ZEN software (Zeiss AG, Jena, Germany). Calculation and quantification of the platelet surface coverage (SC) succeeded using the open-source software ImageJ (V. 1.46r, National Institute of Health, Bethesda, Maryland, USA) analysing five randomly chosen contrast-normalised fields of view at each indicated point in time of each independent experiment. Quantification of the RICM signal intensity was also performed using ImageJ analysing contrast-normalised fields of view at each indicated point in time of each independent experiment, plotted against the time. Mean data of experiments are given with standard deviation (SD). Statistical computation was performed with SAS 9.2

(SAS Institute Inc., Cary, North Carolina, USA). Statistical significance was tested by the unpaired Student's t-test. Significant differences of compared values are indicated by \* ( $P < 0.05$ ).

## Declarations

### Ethics approval and consent to participate

All procedures performed in studies involving human participants were conducted in conformity to the *Declaration of Helsinki* (45) and to *The International Conference on Harmonisation of Technical Requirements for Registration of Pharmaceuticals for Human Use (ICH)* Guidelines (<http://www.ich.org>), accessed in October 2019. This study was approved by the Ethics Committee II of the Heidelberg University (210-245N-MA, Mannheim, Germany). Informed consent was obtained from all individual participants included in the study.

### Consent for publication

Not applicable.

### Availability of data and materials

All data generated or analysed during this study are included in this published article.

### Competing interests

The authors declare that they have no competing interests:

### Funding

The study was funded by the German Research Foundation (DFG) through the projects SFB/Transregio 23 (SWS TP A9) and SHENC - Research Unit FOR1543 (VH/SWS TP A2, MAF/MFS TP B1, RS TP A1 and MFS for a Guest Professorship)

### Authors' contributions

MFS designed and directed research and wrote the manuscript. MAF performed experiments, analysed experimental data and wrote the manuscript. CM developed and performed computational analyses of

the dataset and carried out the statistical evaluation. TO and RS developed, expressed and provided recombinant genetic constructs. AA-K helped in interpreting the biophysical data. SWS directed research and supervised experiments. VH designed and directed research, supervised experiments, analysed experimental data and wrote the manuscript.

## Acknowledgements

Not applicable.

## References

1. Alexander-Katz A, Schneider MF, Schneider SW, Wixforth A, Netz RR. Shear-flow-induced unfolding of polymeric globules. *Physical review letters*. 2006;97(13):138101.
2. Barg A, Ossig R, Goerge T, Schneider MF, Schillers H, Oberleithner H, et al. Soluble plasma-derived von Willebrand factor assembles to a haemostatically active filamentous network. *Thromb Haemost*. 2007;97(4):514-26.
3. Mendolicchio GL, Ruggeri ZM. New perspectives on von Willebrand factor functions in hemostasis and thrombosis. *Semin Hematol*. 2005;42(1):5-14.
4. Ruggeri ZM. Structure of von Willebrand factor and its function in platelet adhesion and thrombus formation. *Best Pract Res Clin Haematol*. 2001;14(2):257-79.
5. Ruggeri ZM. Platelets in atherothrombosis. *Nat Med*. 2002;8(11):1227-34.
6. Ruggeri ZM, Orje JN, Habermann R, Federici AB, Reininger AJ. Activation-independent platelet adhesion and aggregation under elevated shear stress. *Blood*. 2006;108(6):1903-10.
7. Ruggeri ZM. The role of von Willebrand factor in thrombus formation. *Thromb Res*. 2007;120 Suppl 1:S5-9.
8. Sadler JE. Biochemistry and genetics of von Willebrand factor. *Annu Rev Biochem*. 1998;67:395-424.
9. Schneider SW, Nuschele S, Wixforth A, Gorzelanny C, Alexander-Katz A, Netz RR, et al. Shear-induced unfolding triggers adhesion of von Willebrand factor fibers. *Proceedings of the National Academy of Sciences*. 2007;104(19):7899-903.
10. Papi M, Maulucci G, De Spirito M, Missori M, Arcovito G, Lancellotti S, et al. Ristocetin-induced self-aggregation of von Willebrand factor. *Eur Biophys J*. 2010;39(12):1597-603.
11. Campbell V, Marriott K, Stanbridge R, Shlebak A. Successful aortic aneurysm repair in a woman with severe von Willebrand (type 3) disease. *Case Rep Hematol*. 2015;2015:703803.
12. Haberichter SL, Castaman G, Budde U, Peake I, Goodeve A, Rodeghiero F, et al. Identification of type 1 von Willebrand disease patients with reduced von Willebrand factor survival by assay of the VWF propeptide in the European study: molecular and clinical markers for the diagnosis and management of type 1 VWD (MCMDM-1VWD). *Blood*. 2008;111(10):4979-85.

13. Schneppenheim R, Budde U. von Willebrand factor: the complex molecular genetics of a multidomain and multifunctional protein. *Journal of Thrombosis and Haemostasis*. 2011;9:209-15.
14. Kasatkar P, Ghosh K, Shetty S. An atypical manifestation of acquired von Willebrand syndrome (AVWS) associated with systemic lupus erythematosus (SLE). *Ann Hematol*. 2013;93:173-5.
15. Tiede A, Priesack J, Werwitzke S, Bohlmann K, Oortwijn B, Lenting P, et al. Diagnostic workup of patients with acquired von Willebrand syndrome: a retrospective single-centre cohort study. *J Thromb Haemost*. 2008;6(4):569-76.
16. Mannucci PM. von Willebrand factor: a marker of endothelial damage? *Arterioscler Thromb Vasc Biol*. 1998;18(9):1359-62.
17. Moake JL. The role of von Willebrand factor (vWF) in thrombotic thrombocytopenic purpura (TTP) and the hemolytic-uremic syndrome (HUS). *Prog Clin Biol Res*. 1990;337:135-40.
18. Wagner DD. Cell biology of von Willebrand factor. *Annu Rev Cell Biol*. 1990;6:217-46.
19. Springer TA. Biology and physics of von Willebrand factor concatamers. *J Thromb Haemost*. 2011;9 Suppl 1:130-43.
20. Chen H, Fallah MA, Huck V, Angerer JI, Reininger AJ, Schneider SW, et al. Blood-clotting-inspired reversible polymer-colloid composite assembly in flow. *Nat Commun*. 2013;4:1333.
21. Aponte-Santamaria C, Huck V, Posch S, Bronowska AK, Grassle S, Brehm MA, et al. Force-sensitive autoinhibition of the von Willebrand factor is mediated by interdomain interactions. *Biophys J*. 2015;108(9):2312-21.
22. Huck V, Schneider MF, Gorzelanny C, Schneider SW. The various states of von Willebrand factor and their function in physiology and pathophysiology. *Thromb Haemost*. 2014;111(4):598-609.
23. Brehm MA, Huck V, Aponte-Santamaria C, Obser T, Grassle S, Oyen F, et al. von Willebrand disease type 2A phenotypes IIC, IID and IIE: A day in the life of shear-stressed mutant von Willebrand factor. *Thromb Haemost*. 2014;112(1):96-108.
24. Tangelder GJ, Slaaf DW, Arts T, Reneman RS. Wall shear rate in arterioles in vivo: least estimates from platelet velocity profiles. *The American Journal of Physiology*. 1988;254(6 Pt 2):H1059-64.
25. Meyer dos Santos S, Klinkhardt U, Schneppenheim R, Harder S. Using ImageJ for the quantitative analysis of flow-based adhesion assays in real-time under physiologic flow conditions. *Platelets*. 2010;21(1):60-6.
26. De Ceunynck K, Rocha S, Feys HB, De Meyer SF, Uji-i H, Deckmyn H, et al. Local elongation of endothelial cell-anchored von Willebrand factor strings precedes ADAMTS13 protein-mediated proteolysis. *J Biol Chem*. 2011;286(42):36361-7.
27. Back LD, Radbill JR, Crawford DW. Analysis of pulsatile, viscous blood flow through diseased coronary arteries of man. *J Biomech*. 1977;10(5-6):339-53.
28. Goerge T, Kleineruschkamp F, Barg A, Schnaeker EM, Huck V, Schneider MF, et al. Microfluidic reveals generation of platelet-strings on tumor-activated endothelium. *Thromb Haemost*. 2007;98(2):283-6.

29. Huck V, Niemeyer A, Goerge T, Schnaeker EM, Ossig R, Rogge P, et al. Delay of acute intracellular pH recovery after acidosis decreases endothelial cell activation. *J Cell Physiol.* 2007;211(2):399-409.
30. Reininger AJ. Function of von Willebrand factor in haemostasis and thrombosis. *Haemophilia : the official journal of the World Federation of Hemophilia.* 2008;14 Suppl 5:11-26.
31. Riddell AF, Gomez K, Millar CM, Mellars G, Gill S, Brown SA, et al. Characterization of W1745C and S1783A: 2 novel mutations causing defective collagen binding in the A3 domain of von Willebrand factor. *Blood.* 2009;114(16):3489-96.
32. Huck V, Gorzelanny C, Thomas K, Getova V, Niemeyer V, Zens K, et al. From morphology to biochemical state - intravital multiphoton fluorescence lifetime imaging of inflamed human skin. *Sci Rep.* 2016;6:22789.
33. Sing CE, Selvidge JG, Alexander-Katz A. Von Willebrand adhesion to surfaces at high shear rates is controlled by long-lived bonds. *Biophys J.* 2013;105(6):1475-81.
34. Kim J, Zhang CZ, Zhang X, Springer TA. A mechanically stabilized receptor-ligand flex-bond important in the vasculature. *Nature.* 2010;466(7309):992-5.
35. Chen H, Alexander-Katz A. Polymer-based catch-bonds. *Biophys J.* 2011;100(1):174-82.
36. Ju L, Dong JF, Cruz MA, Zhu C. The N-terminal flanking region of the A1 domain regulates the force-dependent binding of von Willebrand factor to platelet glycoprotein Ibalpha. *The Journal of biological chemistry.* 2013;288(45):32289-301.
37. Yago T, Lou J, Wu T, Yang J, Miner JJ, Coburn L, et al. Platelet glycoprotein Ibalpha forms catch bonds with human WT vWF but not with type 2B von Willebrand disease vWF. *The Journal of clinical investigation.* 2008;118(9):3195-207.
38. Yuan H, Deng N, Zhang S, Cao Y, Wang Q, Liu X, et al. The unfolded von Willebrand factor response in bloodstream: the self-association perspective. *J Hematol Oncol.* 2012;5:65.
39. Baldauf C, Schneppenheim R, Stacklies W, Obser T, Pieconka A, Schneppenheim S, et al. Shear-induced unfolding activates von Willebrand factor A2 domain for proteolysis. *Journal of thrombosis and haemostasis : JTH.* 2009;7(12):2096-105.
40. Zhang X, Halvorsen K, Zhang CZ, Wong WP, Springer TA. Mechanoenzymatic cleavage of the ultralarge vascular protein von Willebrand factor. *Science.* 2009;324(5932):1330-4.
41. Casa LD, Deaton DH, Ku DN. Role of high shear rate in thrombosis. *J Vasc Surg.* 2015.
42. Springer TA. von Willebrand factor, Jedi knight of the bloodstream. *Blood.* 2014;124(9):1412-25.
43. Kim J, Hudson NE, Springer TA. Force-induced on-rate switching and modulation by mutations in gain-of-function von Willebrand diseases. *Proc Natl Acad Sci U S A.* 2015;112(15):4648-53.
44. Zilker A, Engelhardt H, Sackmann E. Dynamic Reflection Interference Contrast (Ric-) Microscopy - a New Method to Study Surface Excitations of Cells and to Measure Membrane Bending Elastic-Moduli. *J Phys-Paris.* 1987;48(12):2139-51.
45. Rickham PP. Human Experimentation. Code of Ethics of the World Medical Association. Declaration of Helsinki. *Br Med J.* 1964;2(5402):177.

# Figures

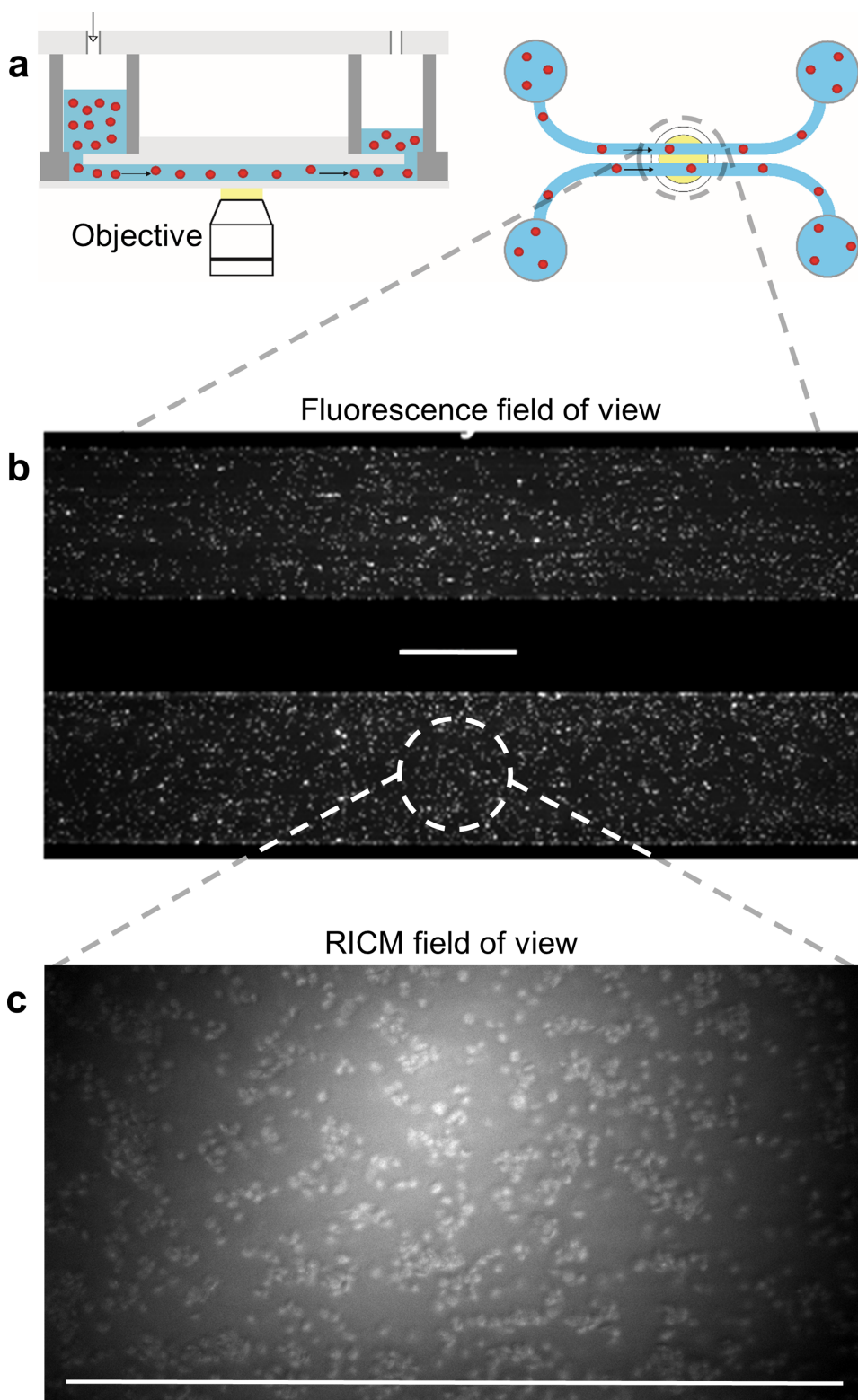


**Figure 1**

Combination of microfluidics and microscopy. (a) Left: A schematic sketch of the pneumatically driven BioFlux flow chamber mounted on the top of the Zeiss Axio Observer microscope, which is operated in fluorescence mode, or reflection interference contrast mode (polarised monochromatic light). Right: Flow

is driven by air pressure from the reservoir into the straight duct. Two channels can be screened simultaneously in the field of view (dashed circle). (b) Fluorescence microscopic image of washed platelets interacting with the footprint of two independent parallel channels under flow conditions. Both channels are coated with wt VWF. (c) RICM image of platelet adhesion in whole blood under flow conditions. The channel is coated with wt VWF. Scale bars correspond to 200  $\mu\text{m}$ .

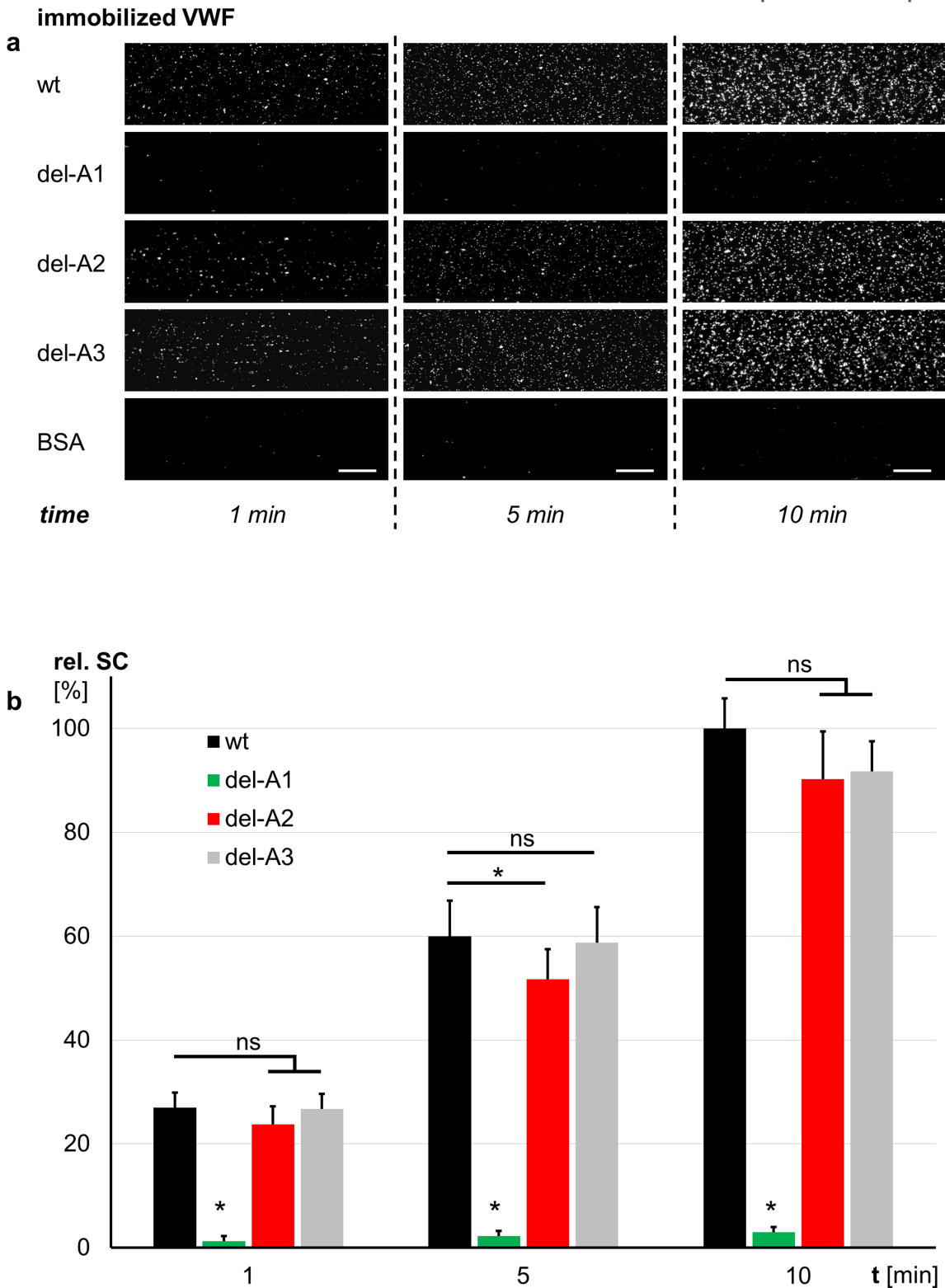
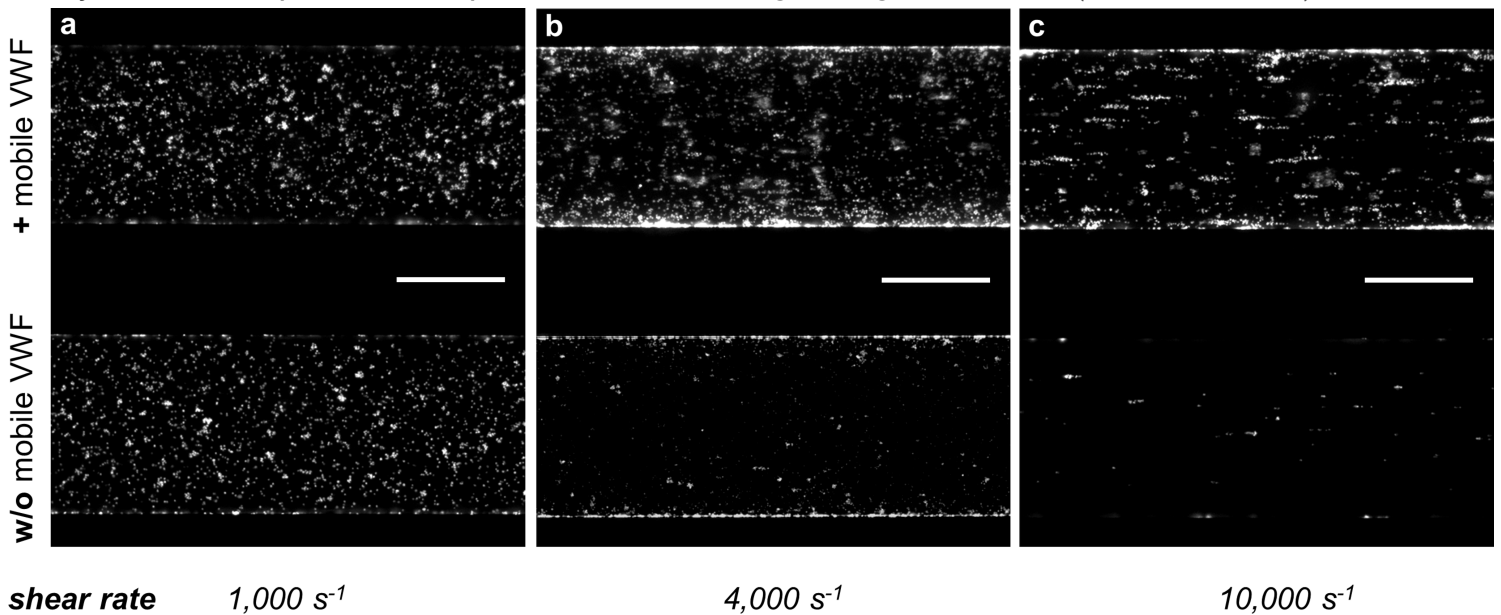


Figure 2

Platelet adhesion on immobilised VWF. (a) After biofunctionalisation of the microfluidic channels with the three different VWF A-domain deletion variants or wt VWF, the adhesion characteristics of platelets are measured upon constant shear rate application of  $500\text{ s}^{-1}$  at indicated points in time. Representative images out of four independent experiments for each group are depicted. As expected, coating with wt VWF leads to an increasing platelet adhesion over time. Del-A1 VWF coating fails to bind platelets. The slight change of platelet adhesion to del-A2 remained negligible compared to the wt VWF. Platelet adhesion to del-A3 coating is similar to wildtype. Biofunctionalisation with BSA serves as negative control. Scale bars correspond to  $100\text{ }\mu\text{m}$ . (b) The relative platelet surface coverage (SC) to wt VWF on indicated biofunctionalisation is plotted against time. Wt VWF (black column), del-A3 (grey column) and del-A2 (red column) show similar platelet adhesion characteristics over time. Del-A1 (green column) nearly fails to bind platelets comparable to BSA serving as negative control (data not shown).



**Figure 3**

Role of soluble VWF in platelet adhesion from low to high shear conditions. Wt VWF biofunctionalised channels are perfused with washed platelets with (+, upper channels) or without (w/o, lower channels) addition of mobile wt VWF at distinct shear rates in the range of  $1,000\text{ s}^{-1}$  to  $10,000\text{ s}^{-1}$ . No differences are found between these experimental groups regarding the platelet SC at low shear rates (a). In contrast, at high shear rates platelets only adhere to the immobilised VWF in the presence of mobile VWF (b, c). Representative images out of five independent experiments for each group. Scale bars correspond to  $200\text{ }\mu\text{m}$ .

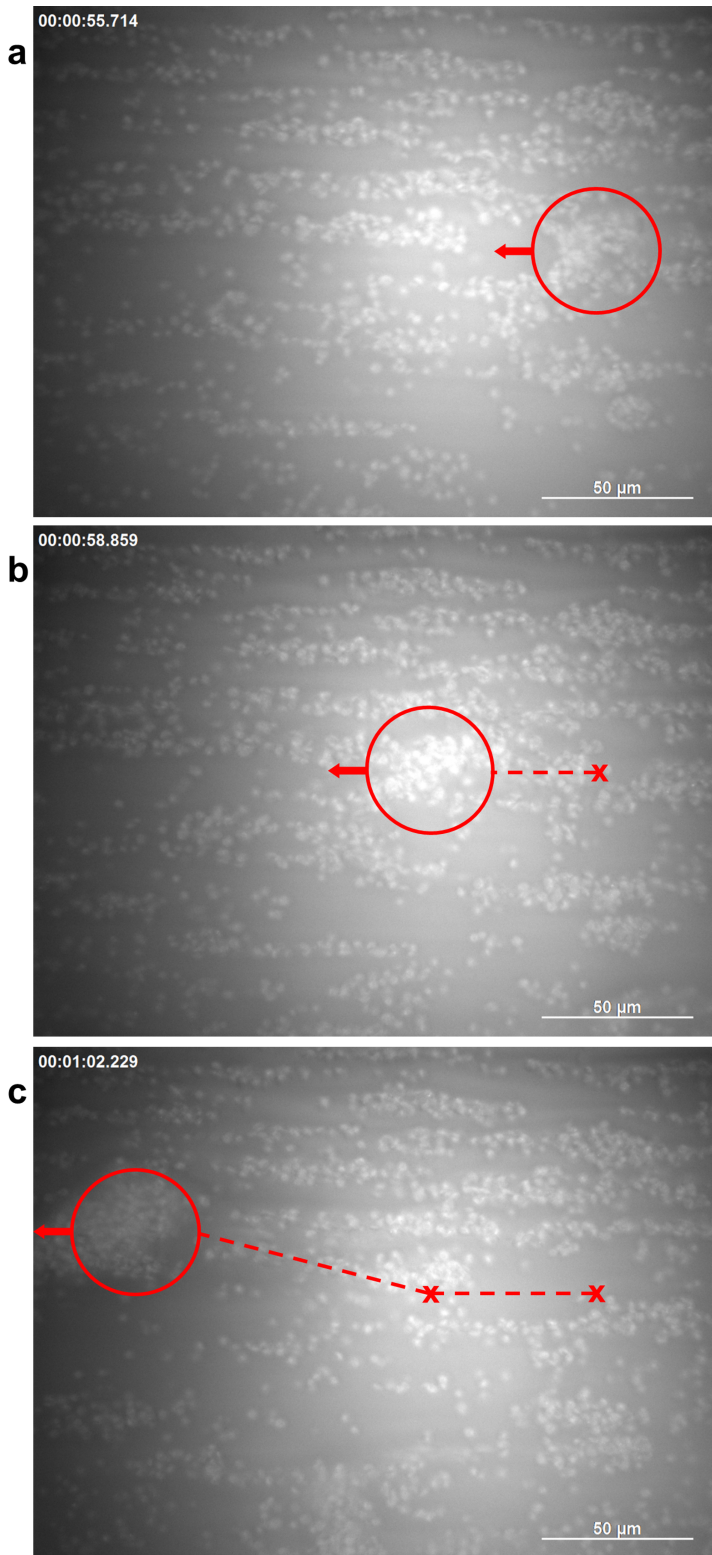


**Figure 4**

The process of aggregate formation on a wt VWF coated channel footprint. An RICM time-lapse live-cell movie (Additional file 1) is recorded at the footprint of a wt VWF biofunctionalised channel perfused with whole blood supplemented with wt VWF. The bright contrasted objects in the focal plane are platelets interacting with VWF at the channel surface. Note that only events in the direct adjacency to the focal plane are visible in RICM. Upon continuously increasing the shear rate within the first 35 seconds, the

pattern of single rolling platelets switches to platelet decorated string-like structures ( $\sim t = 20$  s) which progressively stretch in flow. After some of these strings detach and first aggregates emerge (at the critical shear rate of  $4,000$   $s^{-1}$ ), the flow was stopped leading to an immediate disassembly of strings and aggregates. From  $t = 37$  s, we restart the flow with a constant shear rate of  $4,000$   $s^{-1}$ , resulting in re-formation of aggregates rolling along the surface. Still images at  $t = 56$  s (a),  $t = 59$  s (b) and  $t = 62$  s (c) illustrate the tracking of one exemplarily chosen rolling VWF-platelet aggregate (red circles). Time frame in seconds as indicated, scale bar corresponds to  $50$   $\mu m$ .

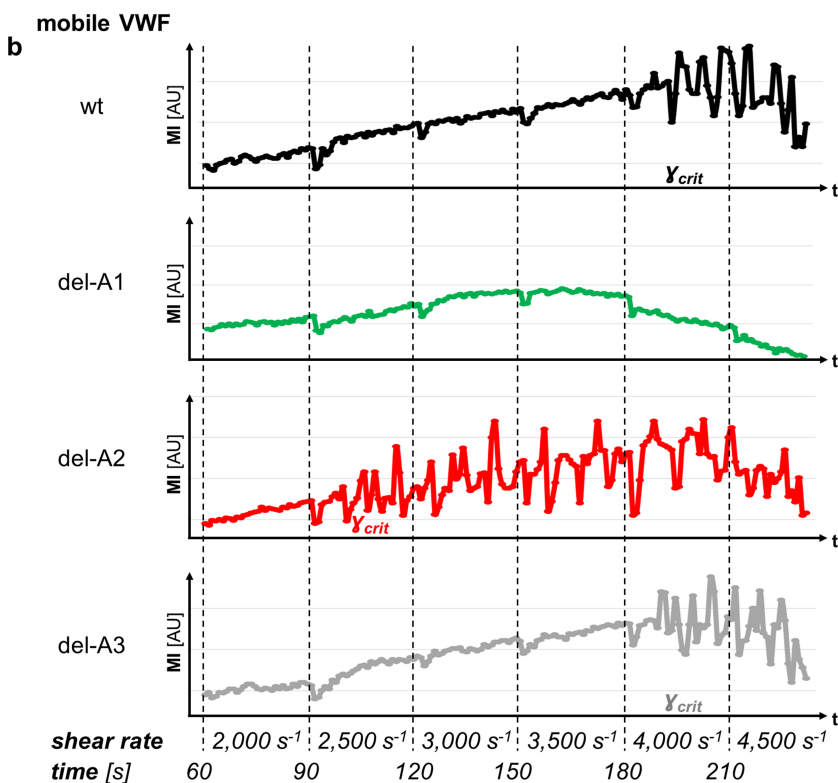
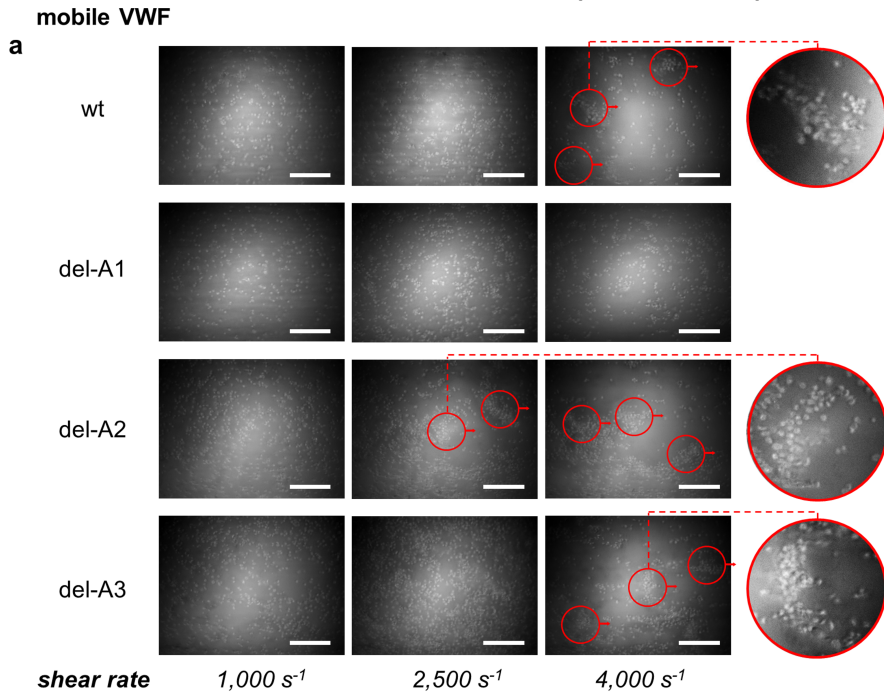
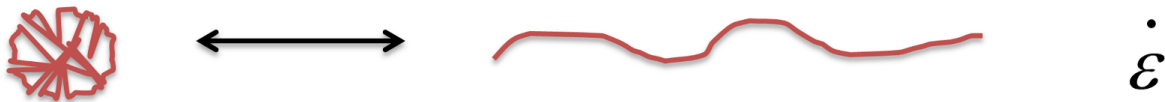


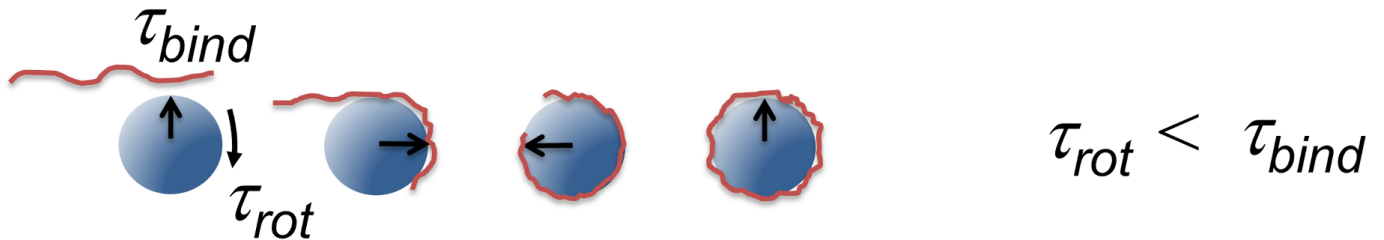
**Figure 5**

Critical shear rate of rolling aggregate formation depends on mobile VWF fraction. After biofunctionalisation with wt VWF, channels are perfused with whole blood supplemented with indicated mobile VWF variant and observed using RICM. The critical shear rate for VWF-platelet aggregate formation is analysed by consecutively increasing the shear from 1,000 s<sup>-1</sup> to 5,000 s<sup>-1</sup>. (a) Whereas the VWF A1-domain deletion completely fails to induce rolling aggregates, del-A2 shows a gain of function by decreasing the critical shear compared to wt VWF; del-A3 does not influence the critical shear rate. Red-arrowed circles illustrate aggregates rolling on the surface in the marked direction. In the right column, magnifications of rolling aggregate regions at the critical shear rate are depicted if available. Scale bars correspond to 50  $\mu\text{m}$ . (b) The RICM signal intensities (MI [AU]) for wt VWF (black line), del-A1 (green line), del-A2 (red line) and del-A3 (gray line) of the VWF-platelet aggregates are plotted against the time, representing distinct shear rates as indicated. Maximum fluctuations in the intensity plots correspond to the critical shear rate  $\dot{\gamma}_{\text{crit}}$ . The analysed  $\dot{\gamma}_{\text{crit}}$  for del-A2 VWF is about 40% less than for wt VWF.

**a**



**b**



**c**

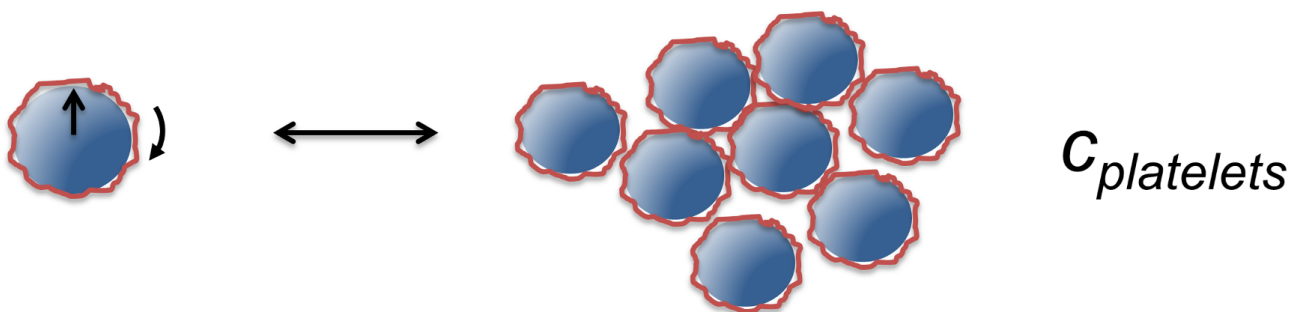


**Figure 6**

Proposed mechanism of aggregate formation. (a) VWF stretching. Conformation of a single VWF molecule changes under high shear flow conditions from globular to elongated form. (b) Cooperative association. Stretched VWF binds to a rotating platelet. Only if the bond-lifetime  $\tau_{\text{bind}}$  is sufficiently long ( $\tau_{\text{bind}} > \tau_{\text{rot}}$ ) compared to the period of rotation  $\tau_{\text{rot}}$ , VWF will begin to “wrap” around the platelet. This will allow forming multiple bounds, which stabilises the association against shear induced bond dissociation. (c) Aggregate formation. Partially VWF coated platelets will cross-interact with further platelets. If the platelet concentration  $c_{\text{platelets}}$  and hence collision rates are sufficient, this will initiate the reversible formation of aggregates.

## Supplementary Files

This is a list of supplementary files associated with this preprint. Click to download.

- [AdditionalFile1.wmv](#)